Title
Thermographic and histological evaluation of laser skin resurfacing scans

Journal
IEEE Journal of Selected Topics in Quantum Electronics, 5(4)

ISSN
1077-260X

Authors
Choi, B
Chan, EK
Barton, JK
et al.

Publication Date
1999

DOI
10.1109/2944.796338

Thermographic and Histological Evaluation of Laser Skin Resurfacing Scans

Bernard Choi, *Student Member, IEEE,* Eric K. Chan, *Member, IEEE,* Jennifer K. Barton, *Associate Member, IEEE,* Sharon L. Thomsen, and Ashley J. Welch, *Fellow, IEEE*

***Abstract*—In general, ablative laser skin resurfacing procedures have shown good short-term efficacy. However, the mechanisms underlying laser skin resurfacing remain poorly understood. We performed a quantitative study to investigate the thermal response of skin to CO_2 laser irradiation. Raster scans were performed on an *in vivo* rat model and radiometric surface temperatures measured using a thermal camera. Temperatures approaching 400 °C were measured during the scans and remained above the initial skin temperature for durations longer than ten seconds. Analysis of histology sections showed that the epidermis remained partially intact after three passes. To explain the observed trends in the temperature response and histology, the dynamics of optical and thermal parameters were investigated. Water vaporization played a key role in governing the response of the skin to subsequent laser passes. Char formation and pulse stacking altered the thermal effects.**

***Index Terms*—Animals, biomedical infrared imaging, laser ablation, pulsed lasers, skin, temperature measurement.**

I. Introduction and Background

A NEW generation of CO_2 resurfacing lasers have been introduced that reportedly vaporize tissue using high-energy short-pulse duration radiation. These clinical laser systems have been studied extensively in animal experiments and human trials [1]–[18].

Although significant improvements in appearance have been reported [3], postoperative complications reduce the efficacy of the wrinkle removal process. The occurrence of scarring is dependent on the depth of thermal damage and on the anatomic location; thin skin (e.g., eyelid, upper lid) is more prone to scarring than other facial areas. As more resurfacing procedures have been performed, the number of reports of scarring incidents has increased significantly [3], [14]. Similar to any type of external wound, areas that are resurfaced are prone to infection. Skin discoloration can be a problem, especially for patients with dark skin [4], [19]; postinflammatory hyperpigmentation can appear anytime from several days to several months postsurgery and last for months or even years. Hypopigmentation occurs less frequently, but some patients do exhibit a lightening of skin color in treated areas. Persistent erythema occurs in nearly all patients and resolves typically in six to eight months.

A more crucial problem is the highly subjective nature of laser resurfacing. Factors that may lead to disappointing results or to serious complications include patient-to-patient variability and the dependence on the surgeon's experience and technique. An operating protocol used successfully by one physician may prove to be inadequate or deleterious with another physician; quantitative explanation of any observed discrepancies is difficult.

These discrepancies are in part because laser-assisted skin resurfacing is a dynamic thermal event governed by the penetration of laser radiation into the tissue and the rate of heat generated by the absorption of the incident laser light. We believe that a better understanding of the optical and thermal response of skin to CO_2 laser radiation will improve our understanding of clinical results. Any framework for analyzing the thermal response of skin to laser irradiation must include the effects of potential dynamic changes in tissue properties during treatment. Absorption of 10.6-μm-wavelength radiation produces a rapid increase in temperature that is a function of the radiant exposure H_o [J/cm^2] of the laser spot and the local optical absorption coefficient μ_a [cm^{-1}]. The skin attributes that may change during the course of pulsed CO_2 laser treatment and subsequently affect the thermal response are discussed below.

A. Dynamic Optical and Thermal Properties

Prior to onset of heat conduction and ablation, the surface temperature rise produced by a laser pulse with radiant exposure H_o is [20]

$$\Delta T = \frac{\mu_a}{\rho c} H_o \tag{1}$$

where ΔT is the local surface temperature rise [°C], ρ is the tissue density [g/cm^3], and c is the specific heat [J/g/°C].

For infrared laser radiation, the primary optical and thermal properties in (1) depend upon the water content of skin [see (2) and (3) below]. The absorption coefficient for 10.6 μm irradiation can be described as

$$\mu_a = W \cdot \mu_{a,\text{water}} + \mu_{a,o} \tag{2}$$

Manuscript received December 14, 1998; revised May 21, 1999. This work was supported by the Office of Naval Research Medical Free Electron Laser Biomedical Science Program under Contract N0014-91-J1564, by the Albert W. and Clemmie A. Caster Foundation, by the Air Force Office of Scientific Research through MURI from DDR&E under Contract F49620-98-1-0480, and by Bio-Medical Consultants, Inc.

B. Choi and A. J. Welch are with the Biomedical Engineering Laser Laboratory, The University of Texas at Austin, Austin, TX 78712 USA.

E. K. Chan is with Indigo Medical, Inc. Cincinnati, OH 45242 USA.

J. K. Barton is with the Biomedical Engineering Program, University of Arizona, Tucson, AZ 85721 USA.

S. L. Thomsen is with the Department of Anatomic Pathology, The University of Texas at Austin MD Anderson Cancer Center, Houston, TX 77030 USA.

Publisher Item Identifier S 1077-260X(99)07520-6.

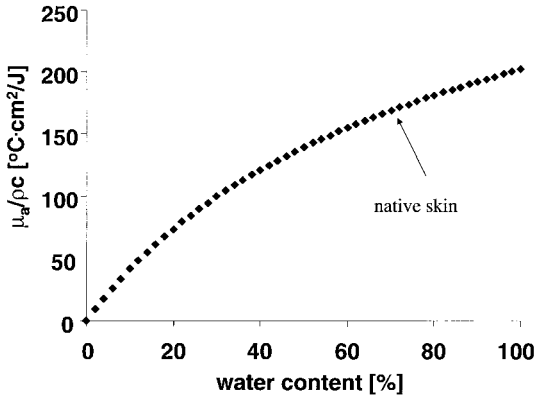

Fig. 1. Plot of $\mu_a/\rho c$ as a function of tissue water content.

TABLE I
OPTOTHERMAL PROPERTIES OF SKIN WITH 70% WATER CONTENT

Parameter	Value
μ_a	594 cm^{-1}
k	$5\cdot10^{-3}$ W/cm/°C
c	3.45 J/g/°C
ρ	1.019 g/cm^3

where W is the water mass content and $\mu_{a,o}$ the water-independent absorption coefficient of skin. $\mu_{a,o}$ represents the absorption coefficient for fully dehydrated skin. In native skin, the water-dependent absorption coefficient is assumed to be sufficiently large to ignore the $\mu_{a,o}$ term in (2); in other words, for fully hydrated skin, $\mu_a = W \cdot \mu_{a,o}$.

The water-content dependence of three key thermal parameters can be described as [21]

$$\rho = (6.16 \cdot 10^{-2} W + 0.938)^{-1} \tag{3a}$$

$$c = 2.5W + 1.7 \tag{3b}$$

$$k = \rho \cdot 10^{-5}(0.454W + 0.174) \tag{3c}$$

where k is the thermal conductivity [W/cm/°C]. Fig. 1 is a plot of the ratio $\mu_a/(\rho c)$ [see (1)] as a function of the tissue water content using (2) and (3a)–(3c). The absorption coefficient of water is assumed to be 848 cm^{-1} at a wavelength of 10.6 μm [21]. It can be seen that an increase in tissue water content results in an increase in $\mu_a/(\rho c)$. Thus, for a situation in which (1) is valid and for a given radiant exposure H_o, irradiation with a laser pulse will result in a higher temperature rise for hydrated than for dehydrated tissue.

The initial water content of viable epidermis and dermis is approximately 70% [22]. The water-content-dependent optical and thermal properties of native skin containing 70% water are listed in Table I.

Note that the temperature change described in (1) represents a maximum value for the peak surface temperature obtained at the end of the laser pulse. If heat conduction, water vaporization, or ablation occur during the pulse, then much of the deposited energy is dissipated and the peak temperature will be much lower than that given by (1).

B. Thermal Diffusion Time

The $1/e$ penetration depth δ of CO_2 laser radiation in skin is about 20 μm. The associated thermal diffusion time τ is

$$\tau = \frac{l^2}{4\alpha} \tag{4}$$

where l is the characteristic length [mm] and α the thermal diffusivity $(\alpha = k/c\rho)$ [cm^2/s]. When spot size diameters are much larger than δ, it can be assumed that $l = \delta$. Using the thermal properties of native skin (Table I), the thermal diffusion time of hydrated skin is approximately 700 μs. This value is much greater than the 100-μs pulsewidth of the laser used in this study; however, there are other factors that lengthen the effective relaxation time beyond 700 μs.

If the laser spot size is much larger than the penetration depth, the laser pulse can be approximated as an instantaneous infinite plane wave [23]. The surface temperature is instantaneously raised to a higher temperature. The temperature decay transient $\Delta T(z,t)$ in degrees Celsius as a function of time t and depth z is described by

$$\Delta T(z,t) = \frac{H_o e^{-(z^2/4\alpha t)}}{2\rho c\sqrt{\pi\alpha t}} \tag{5}$$

The solution of (5) at the $1/e$ penetration depth $(z = \delta)$ and at the corresponding thermal relaxation time $(t = \tau)$ gives

$$\Delta T_\tau = \Delta T\left(z = \delta, t = \frac{\delta^2}{4\alpha}\right) = \frac{H_o}{\rho c\sqrt{\pi \cdot \delta^2}} e^{-1} \tag{6}$$

At $t = 10\tau$, (5) becomes

$$\Delta T_{10\tau} = \Delta T\left(z = \delta, t = 10\frac{\delta^2}{4\alpha}\right) = \frac{H_o}{\rho c\sqrt{10\pi \cdot \delta^2}} e^{-0.1} = 0.78\Delta T_\tau \tag{7}$$

In a similar fashion, it can be found that at $z = \delta$ and $t = 100\tau, \Delta T_{100\tau}$, is equal to $0.35\Delta T_\tau$. Thus, relatively high temperatures will occur at times considerably longer than the commonly cited 695–900-μs diffusion time [24], [25] for CO_2 laser irradiation of skin.

In this paper, we set out to examine and quantify the effects of pulsed CO_2 laser radiation in a series of *in vivo* temperature measurements. The thermal response of skin to irradiation is compared to the extent of subsequent damage depicted in histological sections. The physical results are discussed in terms of dynamic changes that may occur in the optical and thermal parameters of tissue.

II. MATERIALS AND METHODS

In vivo experiments were performed on "Fuzzy" rats (Harlan Sprague Dawley strain) anesthetized with a mixture of Ketamine and Rompun (4 : 3 ratio, 0.1 mL/100 g body weight). The depth of anesthesia was monitored periodically by checking heart rate, breathing rate, and the toe-pinch response. The hair on the backs and flanks of the rats was removed by shaving followed by application of a chemical depilator (Nair, Carter-Wallace, New York, NY).

Anesthetized "Fuzzy" rats were positioned on top of a heating pad. Multiple 3 cm × 3 cm regions were marked on the

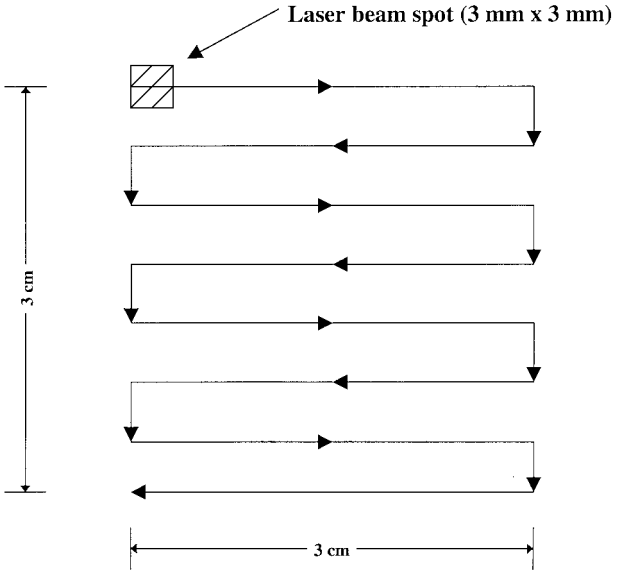

Fig. 2. Sketch of the motion the operator used in performing a given scan. This pattern mimicked that of a recommended clinical treatment. The laser spot size was 3 mm × 3 mm and is represented by the small square on the diagram. Repeat scans began at the same starting point and followed the same pattern.

flanks and irradiated with a TruPulse CO_2 laser system (Tissue Medical Lasers, Albequerque, NM) with a square spot size of 9 mm^2. For the experiments, a pulse duration of 100 μs and a repetition rate of 8 Hz were used. The laser spot was raster scanned in a continuous fashion by moving the handpiece across the skin until the entire 9-cm^2 area was irradiated (Fig. 2). The first row of the raster scan was irradiated by moving the beam from left to right, then the next row was irradiated by moving from right to left, etc. The top portion of the laser handpiece was replaced by a spacer to allow infrared emission from skin to reach the thermal camera. The tip of the spacer was at the focus of the laser beam and the operator attempted to keep it a constant distance from the skin during each scan. Approximately 10 s were required for the completion of each laser pass. Radiant exposures were either 2.4 or 3.9 J/cm^2. A maximum of three raster scans were applied to the same location, and time was provided after each pass (minimum of one minute) to allow the temperature of the irradiated skin to return to a baseline level. The skin was wiped firmly with saline-soaked gauze only after the first pass and not after the second pass. The raster scan pattern, the number of passes, and the wiping protocol were performed in accordance with a recommended clinically used technique.

Surface temperatures were measured during the entire irradiation sequence with a 3–5-μm band-limited thermal camera (Inframetrics Model 600L, Billerica, MA). Images were acquired at standard video rates of 30 frames per second (60 fields per second). The image seen on the video display (i.e., one frame) was actually the combination of two fields separated in time by 16.7 ms. A close-up lens provided a working distance of 9.5 in and a field of view of approximately 3 cm × 3 cm. Internal calibration of the thermal camera compensated for the presence of external optics. The emissivity of human skin was assumed to be 1.0 [26]. Thermal images were recorded with a Super VHS recorder and digitized and processed on a personal computer equipped with a frame grabber.

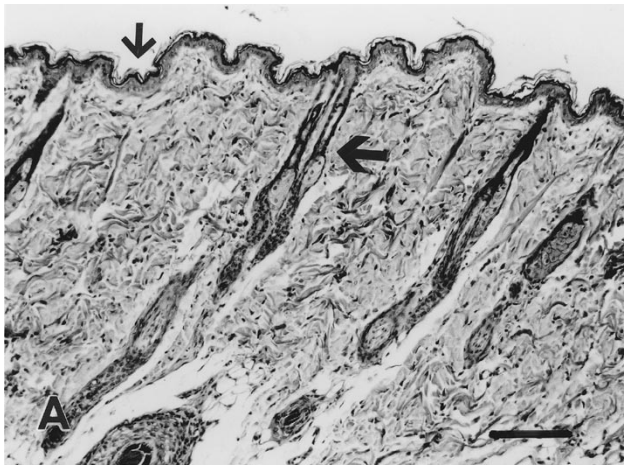

(a)

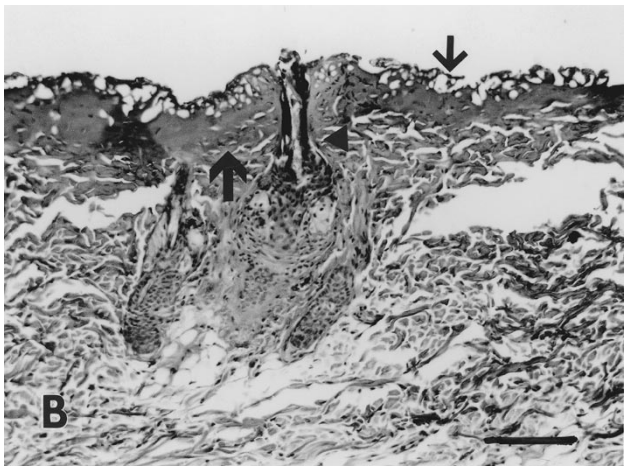

(b)

Fig. 3. (a) Normal rat skin. The thin epidermis (small arrow) covers the dermis composed of collagen fibers that support the hair shafts and sebaceous glands (large arrow), blood vessels (thin black streaks) and cells (small black dots). (b) Thermal Lesion. (Three passes. $H_o = 3.9$ J/cm^2). Only a few remnants of desiccated epidermal fragments (small arrow) remain attached to the exposed coagulated dermal surface. Round water vapor vacuoles distort the epidermis and underlying superficial dermis (large dermal splits are due to tissue sectioning artifact). Thermally induced collagen hyalinization changes the collagen fibers to a dark-staining, glassy (hyaline), amorphous zone at the surface (large arrow points to blue-staining boundary). The normally diagonal hair shaft (arrow head) is pushed upright by contraction of thermally denatured dermal collagen. Cell shrinkage is not identifiable at this magnification. (H&E stains. Original Magnification: 31×. Bar = 100 μm.)

After completion of the experiments, the rats were sacrificed according to procedures stated by The University of Texas at Austin Animal Care and Use Committee. The rat pelts were removed *en bloc*, pinned to a support block, and fixed in 10% buffered formalin. Two representative samples for each set of irradiation parameters were processed for paraffin sectioning; these included a complete cross section of the irradiated region and adjacent normal skin. The 5-μm-thick sections ($n = 5$ per sample) were stained with hematoxylin and eosin (H&E) and Masson's trichrome stains for light (LM) and transmission polarizing microscopy (TPM).

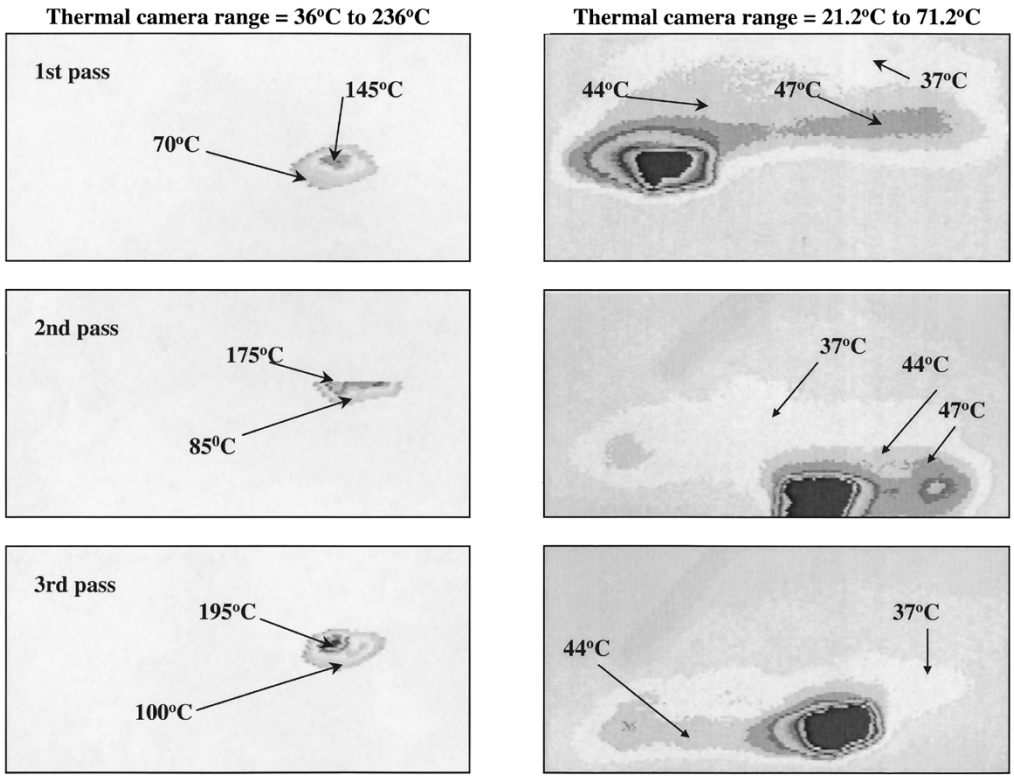

Fig. 4. Representative thermal camera images of pulsed CO_2 laser irradiation (2.4 J/cm^2, 8 Hz) of a 3 cm × 3 cm region on *in vivo* rat skin. Each thermal image was obtained from a different sample. The peak temperatures can be seen in (a), and the residual elevated temperatures from previous pulses can be seen in (b). The image gray levels were inverted to improve image clarity. The rectangular-shaped shadow that can be seen in the images in (b) is the tip of the spacer attached to the laser handpiece (see text for more details).

The following histologic markers of thermal damage were evaluated: 1) epidermal fragmentation and loss; 2) epidermal and dermal vacuolization due to tissue water vaporization; 3) cell and nuclear shrinkage, spindling, and hyperchromasia; and 4) collagen thermal coagulation changes including hyalinization and birefringence loss (Fig. 3).

Water-vapor vacuoles form in tissues as temperatures approach 100 °C. Rapid expansion of superheated steam in the vacuoles will cause explosive fragmentation and loss of desiccated tissue ("popcorn" effect). Individual cell desiccation and thermal coagulation of the cytoskeleton are responsible for cellular shrinkage, spindling, and hyperchromasia. Hyalinization (glass-like appearance) is thermally mediated collagen transformation from distinct fibers to an amorphous sheet of denatured protein. Thermal collagen denaturation also causes loss of the bright birefringence image of native collagen when observed with TPM. All of these histologic changes reflect thermal injury [27].

A zone of collagen hyalinization that stained with a bluish cast in the H&E slides formed the only distinct, measurable border in the dermis. Thermal damage depths marked by this border were measured from the epidermal/dermal junction using a calibrated eyepiece reticule.

III. Results

The mean peak temperatures measured during the raster scans reflect similar trends for both radiant exposures of 2.4 and 3.9 J/cm2 (Table II). Using a t-test, the mean peak temperatures measured during the first and second pass were determined to be equal ($P = 0.49$ for 2.4 J/cm^2, $P = 0.36$ for 3.9 J/cm^2), whereas the peak surface temperatures measured during the third pass were greater than those of the second pass lesions ($P < 0.01$ for both radiant exposures).

TABLE II
MEAN PEAK TEMPERATURES MEASURED DURING RASTER SCANS (MEAN ± SD)

Pass	2.4	3.9
1	219 ± 25°C	335 ± 25°C
	(n = 6)	(n = 8)
2	219 ± 13°C	341 ± 33°C
	(n = 3)	(n = 7)
3	241 ± 10°C	388 ± 7°C
	(n = 3)	(n = 3)

Representative examples of the thermal camera images for each of the three passes are shown for H_o equal to 2.4 J/cm^2 (Fig. 4) and 3.9 J/cm^2 (Fig. 5). The relatively large thermal camera ranges used to obtain peak temperature data from the images depicted in Figs. 4(a) and 5(a) restricted the temperature resolution. Therefore, native sites were irradiated and a second set of images recorded using reduced temperature ranges to resolve small temperature increases at the expense of saturating at high temperatures [Figs. 4(b) and 5(b)]. These

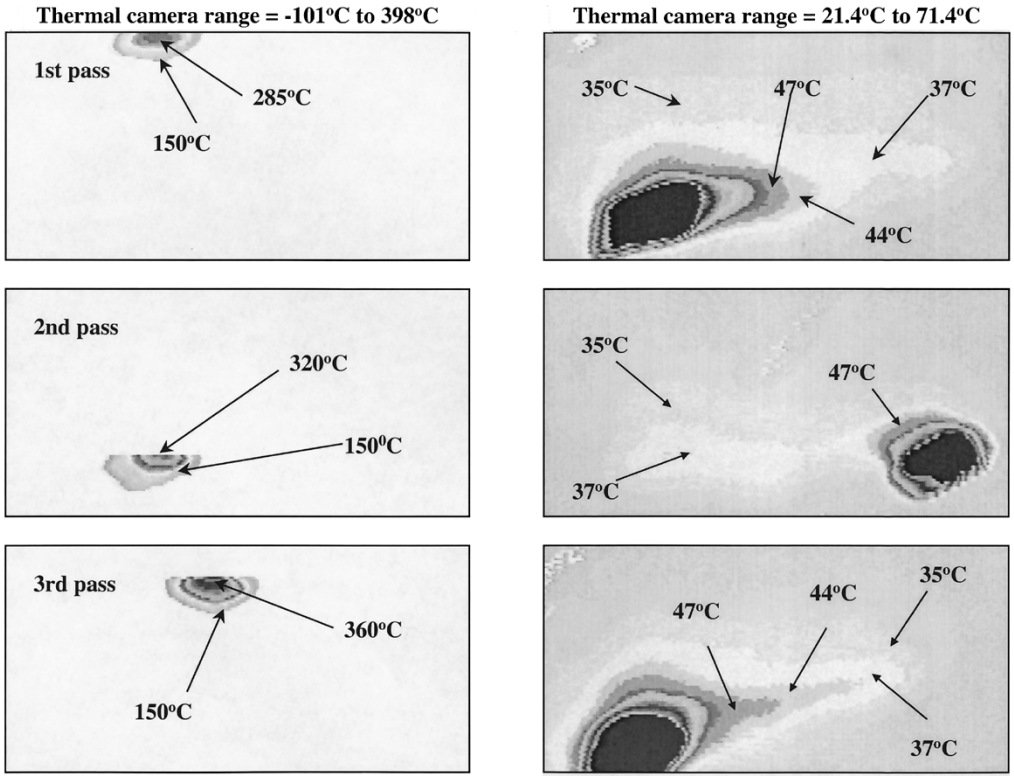

(a) (b)

Fig. 5. Representative thermal camera images of pulsed CO_2 laser irradiation (3.9 J/cm^2, 8 Hz) of a 3 cm × 3 cm region on *in vivo* rat skin. Each thermal image was obtained from a different sample. (a) Peak temperatures. (b) Residual elevated temperatures from previous pulses. The image gray levels were inverted to improve clarity.

images illustrate the temperature decay due to passive skin cooling.

A distinct cracking sound was heard during the first pass for both radiant exposures but was noticeably louder for the 3.9 J/cm^2 pulses. After the first pass, a layer of powdery white debris was seen on the surface of the skin. No char formation was visible on the skin surface.

During the second pass, visible skin contraction occurred immediately after impact of the laser pulses. After irradiation with 2.4-J/cm^2 pulses, focal regions of dark, desiccated tissue were visible; with the 3.9-J/cm^2 pulses, the irradiated areas were covered predominantly with dark, desiccated tissue.

After the third pass, the surface of the skin irradiated at 2.4 J/cm^2 was covered uniformly with brown desiccated tissue, whereas the sites treated at 3.9 J/cm^2 appeared dark brown with small (approximately 1 mm in width) focal regions of black char tissue.

Thermal images of irradiated skin recorded 33 ms [Fig. 6(a)] and approximately 14 s [Fig. 6(b)] after the cessation of irradiation show that temperatures remained elevated for durations on the order of seconds. Skin temperatures just prior to the second and third passes are presented in Fig. 7(a) and (b), respectively. Focal regions with temperatures below baseline (~25 °C) were observed. The magnitude of the subnormal temperatures could not be determined from these images; the white false color represents regions of the target with temperatures below the lowest camera range value (<21.4 °C in this case).

TABLE III
MEAN DEPTHS OF THERMAL DAMAGE. (MEAN ± SD)

Pass	2.4	3.9
1	19 ± 9 μm	39 ± 27μm
	(n = 4)	(n = 4)
2	30 ± 6 μm	61 ± 43 μm
	(n = 4)	(n = 4)
3	33 ± 11 μm	145 ± 60 μm
	(n = 10)	(n = 6)

The depth of thermal damage demarcated by dermal collagen hyalinization was measured from the lesion surface (Table III). For a radiant exposure of 2.4 J/cm^2, the mean depth of thermal damage after the second pass was greater than the value after the first pass ($P<0.05$). However, no statistical difference was found between the second pass and third pass lesions ($P=0.24$). On the other hand, for a radiant exposure of 3.9 J/cm^2, the thermal damage depths measured after the first pass and after the second pass were equal ($P=0.21$), but the thermal damage depth after the third pass was greater than that after the second pass ($P<0.02$). The thermal damage measurements of three-pass, 2.4 J/cm^2 lesions were comparable to one pass, 3.9 J/cm^2 lesions ($P<0.05$).

In general, thermal damage was found in all lesions with the severity and extent increasing with radiant exposure and number of passes (Fig. 8). Water vapor vacuoles and fragmented

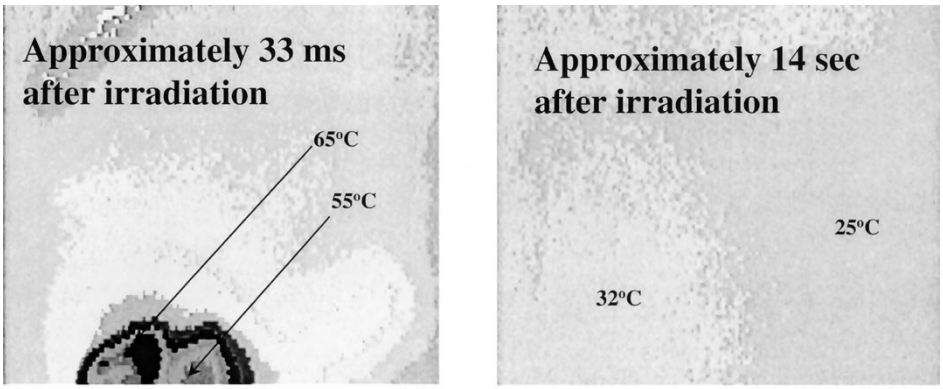

Fig. 6. Thermographic images of skin cooling between passes. A radiant exposure of 3.9 J/cm^2 was used, and the laser was set at a repetition rate of 8 Hz. Images are shown for postirradiation times of approximately (a) 33 ms and (b) 14 s. The temperatures of the last region to be irradiated [as shown in (a)] are still higher than baseline at 14 s. The image gray levels were inverted to improve clarity.

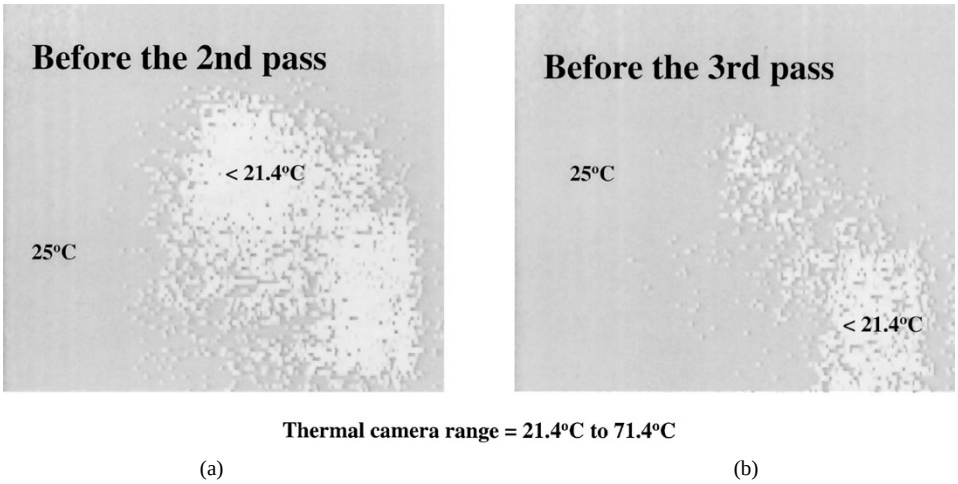

Fig. 7. Skin temperatures just prior to irradiation (3.9 J/cm^2, 8 Hz) with the (a) second and (b) third pass. In both images, focal regions of tissue are below the baseline temperature of 25 °C. The actual temperature of these regions cannot be determined from the obtained images. The image gray levels were inverted to improve clarity.

detachment of the epidermis were present in all lesions with greater epidermal loss in the multiple-pass, higher energy-density lesions. Likewise, the number, size, and extent of dermal steam vacuoles, which were present in all lesions, ranged from a few small, scattered vacuoles in the one-pass, 2.4 J/cm^2 lesions to multiple 30-μm-thick zones of vacuoles in the three-pass, 3.9 J/cm^2 lesions. Epithelial cell shrinkage, spindling, and hyperchromasia were found in the epidermis and superficial adnexa, but no measurable borders were present. These injuries extended deeper into the adnexa with increasing pass number and radiant exposure.

Some thin focal patches of collagen birefringence changes, which occur at higher temperatures than hyalinization, formed in some lesions, but were not measurable. After each of the three passes at 2.4 J/cm^2, hyalinization was present in patches along the lesion surfaces. It was sometimes difficult to distinguish between coagulated and normal tissue. At 3.9 J/cm^2, the band of hyalinization was fairly uniform after each pass.

IV. Discussion

Ablation of skin with CO_2 laser pulses has been studied in several laboratories [15], [22], [28]. Walsh *et al.* [22] used a linear mass loss model to relate their experimental results with theory:

$$D = (H_o - H_{\text{th}})/L \tag{8}$$

where D is the depth of ablation per pulse [cm], H_{th} is the threshold radiant exposure [J/cm^2] required to initiate the ablation process, and L is the heat of ablation [J/cm^3]. From an *in vitro* experiment on guinea pig skin, Walsh *et al.* obtained values of 1.09 and 4.26 kJ/cm^3 for H_{th} and L, respectively.

Using (8), calculated single pulse ablation depths are 3 and 7 μm for radiant exposures of 2.4 and 3.9 J/cm^2, respectively. These depths are in general agreement with incomplete epidermal removal shown in Fig. 8 (first pass) for both radiant exposures. Exact *in vivo* ablation depths for single pulses are difficult to determine for crater depths of only a few microns.

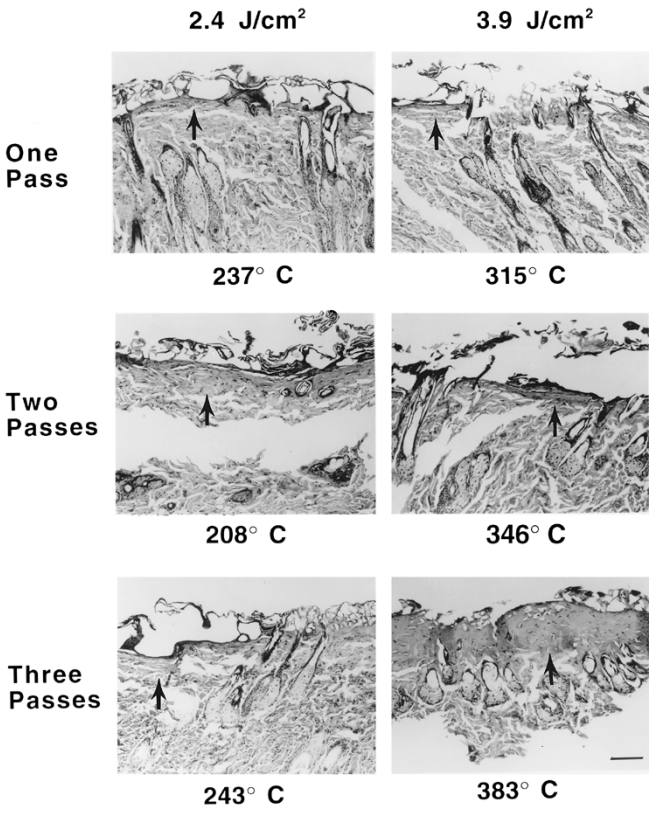

Fig. 8. Thermal lesions in rat skin. Epidermal and dermal water vapor vacuole formation, epidermal fragmentation with detachment, and dermal collagen hyalinization (arrows) become more prominent and uniform with an increased number of laser passes and higher radiant exposures. The large splits in the dermis are artifacts. [H&E stains. Original Magnification: 31×. Bar = 100 μm].

The ablation depths at low radiant exposures reported by Walsh *et al.* [22] are average values for a sequence of 130 pulses.

When ablation occurs, energy provided by the laser pulse must go to: 1) an increase in local tissue temperature; 2) increases in pressure due to tissue water superheating; 3) latent heat of vaporization; and 4) losses associated with heat conduction and the kinetic energy of ablation ejecta.

If all of the energy associated with $H_{\rm th}$ produces sensible heat and there is no heat conduction, the surface temperature associated with the 1.09-J/cm^2 ablation threshold is $T_{\rm th} = 182^\circ$ using (1) and the parameters given in Table I. Threshold temperatures greater than 100 °C indicate tissue-water-vapor superheating and local pressure increases [29].

The mean peak surface temperatures measured during the first pass (Table II) are higher than $T_{\rm th}$. Although the results of this study are insufficient to derive a complete energy balance, qualitative explanations may be useful. Some of the absorbed energy raises the pressure of superheated vapor, increasing both the boiling temperature and the maximum achievable temperature.

Walsh *et al.* [22] irradiated a single spot with multiple pulses; in this study, single pulse was directed to a selected site per scan. As explained in the following section, incidents of pulse overlap occurred during each scan, resulting in increased measured peak temperatures beyond $T_{\rm th}$.

A. Pulse Stacking

The time needed for the skin to cool after the three 3 cm × 3 cm raster scans was on the order of seconds (Fig. 6). The targeted area was divided into 100 disjoint 3 mm × 3 mm subareas. Ideally, each subarea received a single pulse, and the subsequent cooling time would be on the order of 20–40 ms [30] which is consistent with a diffusion time of 700–900 μs for CO_2 laser irradiation of normal tissue. The operator attempted to move the laser in a continuous sweep across the area to minimize overlapping pulses, but superposition of the temperature fields was clearly visible during analysis of the thermal images.

Further evidence of pulse stacking is that during each scan, a wide range of peak temperatures was noted. Some of the peak temperatures shown in Figs. 4(a) and 5(a) have magnitudes which differ by more than one standard deviation from the mean peak values recorded during the raster scans (Table II). We were not able to achieve a consistent measured temperature with each pulse because of the pulse stacking. In reality, the overlapping of pulses led to a wide range of temperatures and regions that required long periods of time [several seconds, as seen in Fig. 6(b)] to return to a baseline temperature.

B. Thermal Response of Skin

CO_2 laser ablation of skin is considered to be largely water dominated [26], [29], [31]–[33]. Although water has a boiling point of 100 °C at atmospheric pressure, peak surface temperatures well above 100 °C were measured in this study; this was due to the rapid superheating of the intracellular water vapor and tissue desiccation. Temperatures associated with ablation are not confined to the boiling temperature of water at atmospheric pressure [29], [31], [33].

After the first pass, the 5-μm thick stratum corneum, which is the skin's main barrier against evaporative water loss [22], [34], was removed and the underlying tissue dehydrated. Another mechanism of water loss was the ablation of water itself; the tissue water served as the target chromophore during CO_2 laser irradiation and eventually boiled off or vaporized during the explosive ablation event. Water evaporation and vaporization led to a decrease in skin water content, and hence target chromophore content; thus, the absorption coefficient decreased and penetration of the laser light increased after ablation had been initiated (2).

The measured peak temperatures during scans (Table II, Figs. 4 and 5) increased very little from the first to the second pass but increased significantly from the second to third pass. The surface of the skin was wiped after the first pass but not after the second pass. Wiping the skin with saline-soaked gauze served to rehydrate the underlying desiccated layers of tissue; the importance of this action will be discussed below.

Although the mean peak temperature measured during the second pass was similar to the value measured during the first pass for both radiant exposures, the peak temperature increased with radiant exposure. The increase in temperature with radiant exposure above the threshold for ablation suggested that a portion of the heat of ablation was sensible heat. The experimentally determined heat of ablation by Walsh *et al.* [22]

of 4.26 kJ/cm^3 was almost twice the latent heat of vaporization of water of 2.25 kJ/cm^3.

If the heat of ablation for the first and second passes are constant and (1) is a valid approximation of the temperature response, then the quantity $\mu_a/(\rho c)$ must be unchanged for the temperature between passes to remain approximately constant.

A lowering in local water content decreases $\mu_a/(\rho c)$ (Fig. 1), which implies that the measured peak temperature between the first and second pass should decrease. By wiping the tissue with saline-soaked gauze after the first pass, the underlying tissue is rehydrated, and the resultant tissue water content during the second pass may be similar to the tissue water content during the first pass. If such is the case, then the peak temperature rise will be similar for the first two passes.

The absence of wiping after the second pass suggests that the peak temperature measured during the third pass should be lower than that measured during the first two passes because the skin was not rehydrated by saline or by any other means. However, our results indicate a marked increase in the measured maximum temperature.

This increase in radiometric surface temperature is related to char formation, which represents burning of tissue and formation of microregions of charcoal. It is known that complete desiccation of skin may result in the formation of char, and there is evidence that this phenomenon is associated with superheating of nucleation sites. Video imaging by Verdaasdonk *et al.* [32] and thermal imaging by Torres [35] indicate nucleation sites that reach 350 °C and ignite during CW argon laser ablation of aorta.

The char that formed had a higher absorption coefficient than that of skin, which resulted in greater absorption of incident laser light [33]. Chylek *et al.* [36] performed studies on mass concentration of carbon particles in the atmosphere. Using 10.6-μm radiation, they derived the following equation for the specific absorption coefficient σ [m^2/s] of carbon as a function of the volume fraction ϕ of carbon particles in the atmosphere

$$\sigma = C(100\phi)^{-D} \tag{9}$$

where C and D are empiricall determined constants ($C = 491, D = 1.98$). By assuming that char consists completely of solid carbon, $\phi = 1.0$; thus, $\sigma = 0.054$ m^2/g for char.

Ishimaru [37] described the following relation for determining μ_a if σ is known

$$\mu_a = C\sigma \tag{10}$$

where C is the molar concentration [mol/L] of the substance of interest. By using the char assumption stated in the previous paragraph, $C \approx \rho$. Assuming that the density of char is approximately that of amorphous carbon ($\rho = 1.95$ g/cm^3 [38]), a char absorption coefficient of 1053 cm^{-1} results, which is almost twice the value of the absorption coefficient of native skin (Table I). The same absorption coefficient can be calculated using (9) and the equations presented by Hale and Querry [39].

The density of charred tissue is approximately one-half the density of native skin ($\rho_{\text{char}} \approx 0.5$ g/cm^3) [40], and

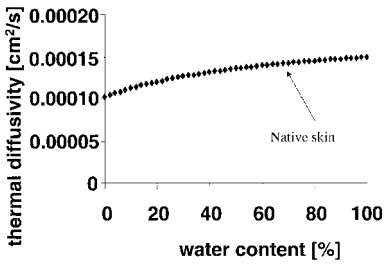

Fig. 9. Plot of thermal diffusivity as a function of tissue water content.

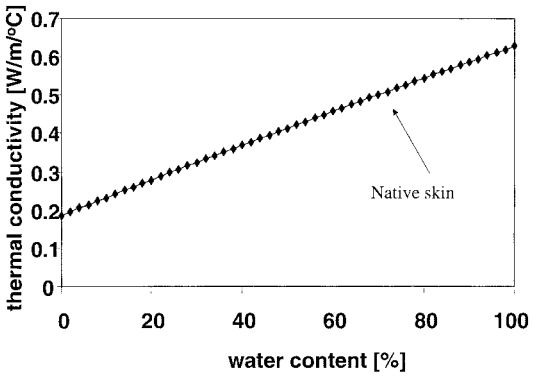

Fig. 10. Plot of thermal conductivity as a function of tissue water content.

the specific heat of char has been estimated to be 0.67 J/g/°C [41], or nearly six times less than the specific heat of normal skin (Table I). A decrease in the heat capacity (equal to ρc) results in a corresponding decrease in the amount of volumetric heat deposition [J/cm^3] required to increase the tissue temperature by 1 °C. The heat capacity of char ($\rho_{\text{char}} c_{\text{char}} \approx 0.34$ J/cm^3/°C) is approximately ten times less than the heat capacity of normal skin (3.52 J/cm^3/°C). Thus, there will be a rapid increase in temperature for a given amount of heat deposition. If the tissue has been dehydrated by previous laser pulses, energy previously required for water vaporization heats the tissue to excessive temperatures of approximately 350 °C. This decreased heat capacity results in a corresponding lowering of thermal diffusivity α [Fig. 9, increased thermal relaxation time (4)], and prolonged periods of increased temperatures.

Thus, in these experiments, desiccated or charred tissue at the surface after the second pass acted as a heat reservoir for subsequent irradiation, which led to a significant increase in tissue surface temperature and finally to an extended zone of thermal necrosis. We hypothesize that the increase in peak surface temperature observed between the second and third passes was due to the presence of desiccated tissue that was not removed prior to the third pass. Rehydration of the skin surface after each pass would minimize or avoid excessively high peak temperatures and subsequent large thermal damage zones.

The relationship between thermal conductivity and tissue water content calculated using (3) is shown in Fig. 10. The decrease in local thermal conductivity due to tissue dehydration has been noted in previous studies [29], [31], [32]. The observed peak temperatures follow closely the events

associated with a decreasing thermal conductivity: as the thermal conductivity decreases, the heat conduction rate to the surrounding tissue decreases, and continued irradiation leads to a rapid increase in the surface temperature until burning and charring events occur [29].

Surface temperatures were monitored prior to each scan. Before the second and third passes, the temperatures of certain regions of the irradiated area were below the baseline temperature of 25 °C (Fig. 7). This temperature depression was noted also by Harris *et al.* [16] during thermal camera measurements of *in vivo* human facial resurfacing. They attributed this phenomenon to the loss of the stratum corneum and subsequent evaporation of extracellular water, which resulted in convective heat loss at the tissue surface. Jaffe and Walsh [34] monitored the surface water flux with an evaporimeter after laser- and scalpel-induced lesions and correlated the decrease in water flux with the reepithelialization of the wounds and found the two measurements to be in good agreement. Thus, quantitative measurements of water flux through the surface of the skin after CO_2 laser resurfacing may provide important insights into the dynamics of CO_2 laser wound healing.

C. Tissue Removal

The results of Walsh and Deutsch [22] suggest that a radiant exposure well over 20 J/cm^2 would be required to remove the complete epidermis (65 μm) with the first laser pass; clinically, radiant exposures range between 3.5–7.1 J/cm^2 [15]. Thus, ablation cannot be the only mechanism involved in determining the total resurfacing depth.

In this study, ablation depths at low radiant exposures could not be identified conclusively from an acute histological analysis; removal of epidermal tissue may have been due to tissue dehydration effects, ablation, or both. Ultimately, the injured tissue sloughs off, and the depth of damage is determined in chronic wound healing studies [42]. However, the results of our study indicate that three passes of 3.9 J/cm^2 did not remove the epidermis entirely even after wiping with saline-soaked gauze. This is in stark contrast to studies detailing complete epidermal removal after the first pass and subsequent removal of dermal tissue with additional passes [13], [43], [44].

Wiping the skin with saline-soaked gauze after the first pass may remove all or part of the dried, fragmented epidermis that has detached from the underlying dermis. Using low radiant exposures, a natural split at the dermal-epidermal junction can be induced [2]. The values necessary to induce this split are heretofore unknown, but if this cleavage of the junction occurs with clinically used radiant exposures, then removal of the epidermis with gauze would be relatively easy. However, in our experiments, this natural split was not observed.

D. Collagen Contraction

Optimal laser parameters can be accurately determined only if the actual mechanisms underlying CO_2 laser skin resurfacing can be elucidated. Heat-induced collagen contraction is probably one mechanism. During the second pass, we have observed a definite contraction of the skin. Contraction has been associated with gross observations of ablation of the dermal portion of skin [4], but thermally induced collagen contraction is due solely to denaturation of collagen proteins and dehydration of the tissue.

A study by Lask *et al.* [17] has examined the use of cryogen spray cooling and laser irradiation for inducing collagen contraction in the dermis without removing the epidermis. The results of our study have demonstrated that collagen contraction is possible without removing the entire epidermis. Collagen contraction is estimated to occur at temperatures of 55 °C–62 °C [45] and results in tissue contraction. Therefore, heat conducted from the irradiation site to the dermis probably is responsible for the perceived contraction of the skin.

V. Conclusion

In summary, during clinically based raster scans of pulsed CO_2 laser skin irradiation, peak temperatures approaching 400 °C were measured. The importance of wiping with wet gauze after each pass was stressed; the moisture from the gauze rehydrated the underlying surface layer and thus partially restored the target chromophore at 10.6 μm. Although the time between pulses was greater than the thermal relaxation time of the skin, temperature superposition effects were apparent due to pulse stacking during laser skin resurfacing scans. The net result of elevated temperatures was an extended zone of thermal necrosis, which could lead ultimately to an increased risk of scarring and delayed wound healing.

It is extremely important that the clinician chooses an appropriate repetition rate to avoid pulse overlap. Lasers equipped with computer-pattern generators operate by overlapping pulses during a single scan; the ablation rate and thermal damage zones of these lasers require further study.

Acknowledgment

The authors thank Tissue Medical Lasers for providing the laser system, and Drs. T. Milner, J. Walsh, D. Harris, and S. Jacques for their insightful comments and suggestions.

References

[1] B. S. Biesman, "Cutaneous facial resurfacing with the carbon dioxide laser," *Ophthal. Surg. Lasers*, vol. 27, pp. 685–698, 1996.
[2] R. E. Fitzpatrick and M. P. Goldman, "Advances in carbon dioxide laser surgery," *Clin. Dermatol.*, vol. 13, pp. 35–47, 1995.
[3] G. J. Hruza and J. S. Dover, "Laser skin resurfacing," *Arch Dermatol.*, vol. 132, pp. 451–455, 1996.
[4] R. E. Fitzpatrick, M. P. Goldman, N. M. Satur, and W. D. Tope, "Pulsed carbon dioxide laser resurfacing of photoaged facial skin," *Arch Dermatol.*, vol. 132, pp. 395–402, 1996.
[5] D. B. Apfelberg, "The ultrapulse carbon dioxide laser with computer pattern generator automatic scanner for facial cosmetic surgery and resurfacing," *Ann. Plast. Surg.*, vol. 36, pp. 522–529, 1996.
[6] T. S. Alster, "Comparison of two high-energy, pulsed carbon dioxide lasers in the treatment of periorbital rhytides," *Dermatol. Surg.*, vol. 22, pp. 541–545, 1996.
[7] N. J. Lowe, G. Lask, and M. E. Griffin, "Laser skin resurfacing: Pre- and posttreatment guidelines," *Dermatol. Surg.*, vol. 21, pp. 1017–1019, 1995.
[8] N. J. Lowe, G. Lask, M. E. Griffin, A. Maxwell, P. Lowe, and F. Quilada, "Skin resurfacing with the Ultrapulse carbon dioxide laser: Observations on 100 patients," *Dermatol. Surg.*, vol. 21, pp. 1025–1029, 1995.
[9] L. M. David, A. J. Sarne, and W. P. Unger, "Rapid laser scanning for facial resurfacing," *Dermatol. Surg.*, vol. 21, pp. 1031–1033, 1995.

[10] G. Chernoff, M. Slatkine, E. Zair, and D. Mead, "SilkTouch: A new technology for skin resurfacing in aesthetic surgery," *J. Clin. Laser Med. Surg.*, vol. 13, pp. 97–100, 1995.
[11] C. Weinstein, "Ultrapulse carbon dioxide laser removal of periocular wrinkles in association with laser blepharoplasty," *J. Clin. Laser Med. Surg.*, vol. 12, pp. 205–209, 1994.
[12] J. Cotton, A. F. Hood, R. Gonin, W. H. Beeson, and C. W. Hanke, "Histologic evaluation of preauricular and postauricular human skin after high-energy, short-pulse carbon dioxide laser," *Arch Dermatol.*, vol. 132, pp. 425–428, 1996.
[13] R. E. Fitzpatrick, W. D. Tope, M. P. Goldman, and N. M. Satur, "Pulsed carbon dioxide laser, trichloroacetic acid, Baker-Gordon phenol, and dermabrasion: A comparative clinical and histologic study of cutaneous resurfacing in a porcine model," *Arch Dermatol.*, vol. 132, pp. 469–471, 1996.
[14] E. V. Ross, R. D. Glatter, D. Duke, and J. M. Grevelink, "Effects of overlap and pass number in CO_2 laser skin resurfacing: Preliminary results of residual thermal damage, cell death, and wound healing," *Proc. SPIE*, vol. 2970, pp. 395–405, 1997.
[15] E. V. Ross, Y. Domankevitz, M. Skrobal, and R. R. Anderson, "Effects of CO_2 laser pulse duration in ablation and residual thermal damage: Implications for skin resurfacing," *Lasers Surg. Med.*, vol. 19, pp. 123–129, 1996.
[16] D. M. Harris, D. S. Fried, L. Reinisch, T. Bell, and R. Lyver, "Thermal measurements of short duration CO_2 laser resurfacing," *Proc. SPIE*, vol. 2970, pp. 319–326, 1997.
[17] G. Lask, P. K. Lee, M. Seyfzadeh, J. S. Nelson, T. E. Milner, B. Anvari, D. Dave, R. G. Geronemus, L. J. Bernstein, H. Mittlelman, L. A. Ridener, W. F. Coulson, B. Sand, J. Baumgardner, D. Hennings, R. Menefee, and M. Berry, "Nonablative laser treatment of facial rhytides," *Proc. SPIE*, vol. 2970, pp. 338–349, 1997.
[18] G. Lask, G. Keller, N. Lowe, and D. Gormley, "Laser skin resurfacing with the SilkTouch flashscanner for facial rhytides," *Dermatol. Surg.*, vol. 21, pp. 1021–1024, 1995.
[19] C. Ho, Q. Nguyen, N. J. Lowe, M. E. Griffin, and G. Lask, "Laser resurfacing in pigmented skin," *Dermatol. Surg.*, vol. 21, pp. 1035–1037, 1995.
[20] R. R. Anderson and J. A. Parrish, "Selective photothermolysis: Precise microsurgery by selective absorption of pulsed radiation," *Science*, vol. 220, pp. 524–527, 1983.
[21] M. J. P. Brugmans, J. Kemper, G. H. M. Gijsbers, F. W. van der Meulen, and M. J. C. van Gemert, "Temperature response of biological materials to pulsed nonablative CO_2 laser irradiation," *Lasers Surg. Med.*, vol. 11, pp. 587–594, 1991.
[22] J. T. Walsh and T. F. Deutsch, "Pulsed CO_2 laser tissue ablation: Measurement of the ablation rate," *Lasers Surg. Med.*, vol. 8, pp. 264–275, 1988.
[23] H. S. Carslaw and J. C. Jaeger, *Conduction of Heat in Solids*. Oxford, U.K.: Clarendon, 1959.
[24] R. E. Fitzpatrick, M. P. Goldman, and J. Ruiz-Esparza, "Clinical advantage of the CO_2 laser superpulsed mode: Treatment of verruca vulgaris, seborrheic keratoses, lentigines, and actinic cheilitis," *J. Dermatol. Surg. Oncol.*, vol. 20, pp. 449–456, 1994.
[25] J. T. Walsh, T. J. Flotte, R. R. Anderson, and T. F. Deutsch, "Pulsed CO_2 laser tissue ablation: Effect of tissue type and pulse duration on thermal damage," *Lasers Surg. Med.*, vol. 8, pp. 108–118, 1988.
[26] J. A. Pearce, A. J. Welch, M. Motamedi, and R. Agah, "Thermographic measurement of tissue temperature during laser angioplasty," in *Heat and Mass Transfer in the Microcirculation of Thermally Significant Vessels*, 1986, pp. 49–54.
[27] J. Pearce and S. Thomsen, "Rate process analysis of thermal damage," in *Optical-Thermal Response of Laser-Irradiated Tissue*, A. J. Welch and M. J. C. van Gemert, Eds. New York: Plenum, 1995.
[28] A. L. McKenzie, "How far does thermal damage extend beneath the surface of CO_2 laser incisions?" *Phys. Med. Biol.*, vol. 28, pp. 905–912, 1983.
[29] A. J. Welch, M. Motamedi, S. Rastegar, G. L. LeCarpentier, and E. D. Jansen, "Laser thermal ablation," *Photochem Photobiol.*, vol. 53, pp. 815–823, 1991.
[30] B. Choi, J. K. Barton, E. K. Chan, and A. J. Welch, "Imaging of the irradiation of skin with a clinical CO_2 laser system: Implications for laser skin resurfacing," *Lasers Surg. Med.*, vol. 23, pp. 185–193, 1998.
[31] G. L. LeCarpentier, M. Motamedi, L. P. McMath, S. Rastegar, and A. J. Welch, "Continuous wave laser ablation of tissue: Analysis of thermal and mechanical events," *IEEE Trans. Biomed. Eng.*, vol. 40, pp. 188–200, 1993.
[32] R. M. Verdaasdonk, C. Borst, and M. J. C. van Gemert, "Explosive onset of continuous wave tissue ablation," *Phys. Med. Biol.*, vol. 35, pp. 1129–1144, 1990.
[33] T. G. van Leeuwen, E. D. Jansen, M. Motamedi, C. Borst, and A. J. Welch, "Pulsed laser ablation of soft tissue," in *Optical-Thermal Response of Laser-Irradiated Tissue*, A. J. Welch and M. J. C. van Gemert, Eds. New York: Plenum, 1995.
[34] B. H. Jaffe and J. T. Walsh, "Water flux from partial-thickness skin wounds: Comparative study of the effects of Er:YAG and Ho:YAG lasers," *Lasers Surg. Med.*, vol. 18, pp. 1–9, 1996.
[35] J. H. Torres, M. Motamedi, and A. J. Welch, "Disparate absorption of argon laser radiation by fibrous versus fatty plaque: Implications for laser angioplasty," *Lasers Surg. Med.*, vol. 10, pp. 149–157, 1990.
[36] P. Chylek, V. Ramaswamy, R. Cheng, and R. G. Pinnick, "Optical properties and mass concentration of carbonaceous smokes," *Appl. Opt.*, vol. 20, pp. 2980–2985, 1981.
[37] A. Ishimaru, *Single Scattering and Transport Theory*. San Diego, CA: Academic, 1978.
[38] F. P. Incropera and D. P. DeWitt, *Fundamentals of Heat and Mass Transfer*. New York: Wiley, 1996.
[39] G. M. Hale and M. R. Querry, "Optical constants of water in the 200-nm to 200-μm region," *Appl. Opt.*, vol. 12, pp. 555–563, 1973.
[40] M. Gerstmann, Y. Linenberg, A. Katzir, and S. Akselrod, "Char formation in tissue irradiated with a CO_2 laser: Model and simulations," *Opt. Eng.*, vol. 33, pp. 2343–2351, 1994.
[41] F. A. Duck, *Physical Properties of Tissue: A Comprehensive Reference Book*. London, U.K.: Academic, 1990.
[42] S. Thomsen, B. Baldwin, E. Chi, J. Ellard, and J. Schwartz, "Histopathology of laser skin resurfacing," *Proc. SPIE*, vol. 2970, pp. 287–293, 1997.
[43] T. S. Alster, A. N. B. Kauvar, and R. G. Geronemus, "Histology of high-energy pulsed CO_2 laser resurfacing," *Semin. Cutan. Med. Surg.*, vol. 15, pp. 189–193, 1996.
[44] K. J. Smith, H. G. Skelton, J. S. Graham, T. A. Hamilton, B. E. Hackley, Jr., and C. G. Hurst, "Depth of morphologic skin damage and viability after one, two, and three passes of a high-energy short-pulse CO_2 laser (Tru-Pulse) in pig skin," *J. Amer. Acad. Dermatol.*, vol. 37, pp. 204–210, 1997.
[45] H. Stringer and J. Parr, "Shrinkage temperature of eye collagen," *Nature*, vol. 204, p. 1307, 1964.

Bernard Choi (S'98) was born in Elk Grove, IL, on September 3, 1974. He received the B.S. degree from Northwestern University in 1996 and the M.S. degree from The University of Texas at Austin in 1998, all in biomedical engineering. He is currently working toward the Ph.D. degree in biomedical engineering at The University of Texas at Austin.

His research interests include infrared thermographic techniques, therapeutic applications of lasers in dermatology, laser-induced collagen contraction, and cryogen spray cooling.

Eric K. Chan (M'98) received the B.S. and M.S. degrees from the Institute of Optics at the University of Rochester, Rochester, NY, and the doctoral degree in biomedical engineering from the University of Texas at Austin in 1997.

He gained professional experience in optical engineering from working at Xerox Corporation, IBM Thomas J. Watson Research Center, and Bausch & Lomb, Inc. In the course of his graduate studies, he worked on a number of research areas including laser tissue soldering, laser skin resurfacing, modeling of laser-tissue interaction and characterization of tissue optical properties. Currently, he is with the Research and Development Group at Indigo Medical, Inc., a Johnson & Johnson company specialized in developing novel devices for urologic disorders. His research interests include interstitial laser heating of tissues and minimally invasive surgery. He has authored and co-authored over 25 peer-reviewed and conference proceeding papers.

Dr. Chan is a Fellow of the ASLMS and a member of the International Society for Optical Engineering (SPIE), and Optical Society of America. He is also a member of Tau Beta Pi and Phi Kappa Phi.

Jennifer K. Barton (S'95–A'98) received the B.S. degree from the University of Texas at Austin and the M.S. degree from the University of California at Irvine, both in electrical engineering, and the Ph.D. degree in biomedical engineering from the University of Texas at Austin in 1998.

She joined the University of Arizona as an Assistant Professor of biomedical engineering in 1998. Her research interests include laser therapeutics, laser-tissue modeling, and optical coherence tomography.

Sharon L. Thomsen received the A.B. degree from the University of Washington, Seattle, and and the M.D. degree from Stanford University, Stanford, CA.

She did her residency in Anatomic Pathology at the University of Chicago. She has been on the Pathology faculties at the University of Chicago, and University of Miami and is now Associate Professor of Anatomic Pathology at the University of Texas M. D. Anderson Cancer Center. Her research interests have centered upon using qualitative and quantitative pathologic techniques to investigate the interactions of nonionizing electromagnetic radiation on biologic tissues with emphasis on light transport and thermal effects.

Ashley J. Welch (M'66–SM'79–F'91), for photograph and biography, see this issue, p. 1082.